A rapid microwave approach for 'one-pot' synthesis of antibiotic conjugated silver nanoparticles with antimicrobial activity against multi-drug resistant bacterial pathogens

Juwon S. Afolayan, Adam M. Varney, Jonathan C. Thomas, Samantha McLean, and Carole C. Perry**

All authors are affiliated with: School of Science and Technology, Nottingham Trent University, Clifton Lane, Nottingham, NG11 8NS, UK.

Corresponding Authors

*Professor Carole C. Perry: carole.perry@ntu.ac.uk and Dr Samantha McLean: Samantha.mclean@ntu.ac.uk

Highlights

- Active ampicillin-Ag nanoparticles can be made by a microwave synthesis approach
- Antibacterial properties of ampicillin-Ag nanoparticles can be tuned by synthesis method
- Ampicillin-Ag nanoparticles have increased antimicrobial activity against MDR bacteria compared to ampicillin or Ag nanoparticles alone
- Ampicillin antibacterial activity can be rejuvenated on conjugation with Ag NPs
- A one-pot synthesis approach yields ampicillin-Ag NPs potent against MDR bacteria

Abstract

Deaths directly attributable to drug-resistant infections reached 1.27 million in 2019 and continue to rise. This escalating resistance to antibiotics has driven a resurgence in the exploration of ancient antimicrobials to develop efficacious alternatives. The modern field of nanomaterials is a promising area of research with silver nanoparticles performing well as antimicrobial agents due to their large surface area and multiple bacterial targets. In the current study antibiotic conjugated silver nanoparticles (3 - 35 nm) were synthesized using β-lactam antibiotic, ampicillin. The method of heating during synthesis either microwave (4 mins.) or convection (4 hrs.) influenced the physical characteristics of the ampicillin coated silver nanoparticles, however both approaches produced nanomaterials with antimicrobial activity against a variety of multi-drug resistant (MDR) clinical isolates in physiologically relevant media (when present at <0.2-2.28 mg L^{-1} in defined media). Critically, the microwave method is five times faster than the traditional water bath method, allowing rapid synthesis of ampicillin-conjugated nanoparticles, which supports scale up processes for industry. We suggest that the combination of antibiotic and silver in these nanoparticles produces a synergistic effect that circumvents resistance mechanisms and has the potential to provide a new line of combinatorial agents able to treat multi-drug resistant infections.

Graphical abstract

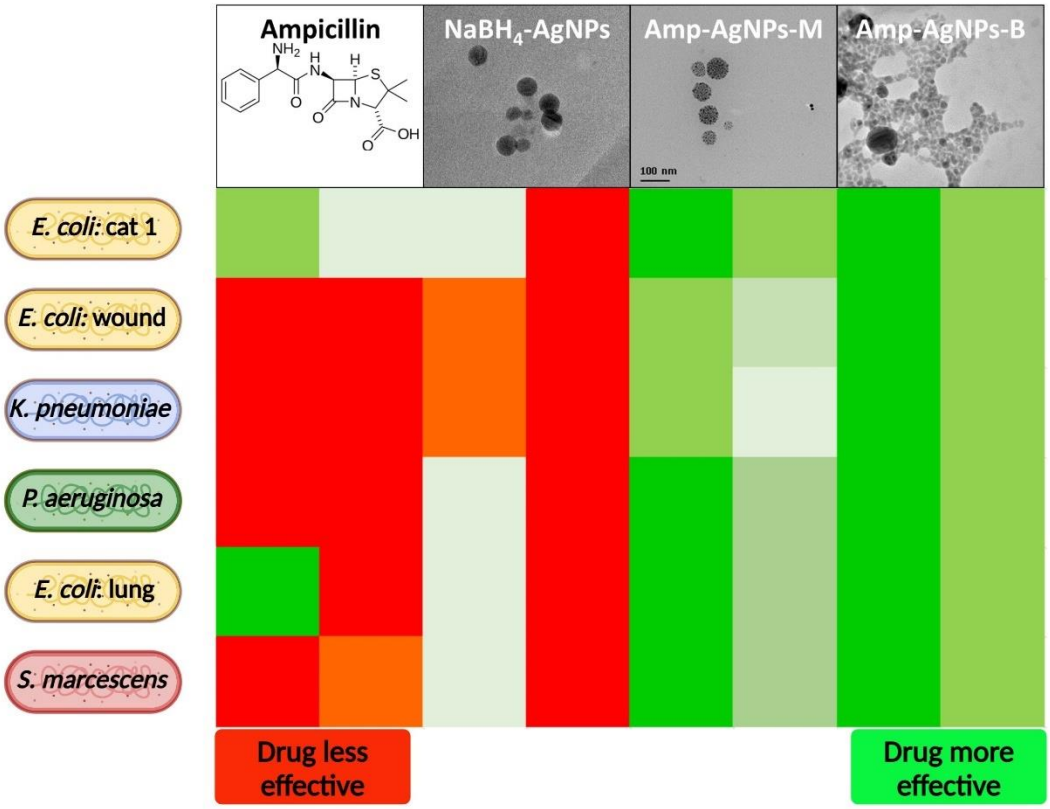

Keywords: silver, nanoparticles, nanosilver, antimicrobials, antimicrobial resistance, drug development

1. Introduction

Silver has been used for its antibacterial activity throughout history [1]; aqueous silver nitrate ($AgNO_3$) was used as long ago as the 1800's to prevent the transmission of *Neisseria gonorrhoeae* from infected mothers to children during childbirth [2]. However, the golden age of antibiotic discovery and development slowed the use of silver as an antimicrobial in favor of highly effective antibiotics that demonstrate selective toxicity. Use of antibiotics such as ampicillin increased dramatically from the early 1940's, and over time this gave rise to the evolution of antibiotic resistance [3]. In the modern world, many bacterial pathogens are multi-drug resistant, with some exhibiting pan-drug resistance, meaning they are not susceptible to any clinically available drug. However, the antibiotic development pipeline is fragile and failing, with a recent report concluding that "the breadth and novelty of the clinical antibiotic pipeline is insufficient to meet the growing threat of antibiotic resistant pathogens" [4]. The issue of antibiotic development is further compounded by the financial risks involved; large pharmaceutical companies are hesitant to invest in antibiotic development due to the lack of financial incentives for development of drugs of this type. Even with a suite of push-pull incentives being developed by governments globally to encourage growth in this sector, the risks are currently too great to drive investment [5]. Furthermore, the cost of new antibiotics entering the market makes then a non-viable option for lower- middle-income countries that experience some of the highest incidences of antibiotic resistance [6].

The increasing threat of antibiotic resistance and fragile antibiotic pipeline has driven researchers to search for new lower risk cost effective methods of treating infections including revisiting known antimicrobial metals such as silver [7]. Due to their superior efficacy compared to bulk materials, the antibacterial properties of silver nanoparticles (AgNPs) are currently being explored for various biomedical applications [8] and it has been suggested that conjugating antibiotics to nanoparticles may circumvent some antibiotic resistance mechanisms, improving the efficacy of cheap antibiotics that are little or no longer used.This opens the door to reintroducing older antibiotics already approved for human use as a viabletreatment for where resistance has evolved amongst bacterial populations but at a fraction of the cost of developing antibiotics. One such antibiotic-nanosilver combination is ampicillin conjugated to AgNPs. Ampicillin, a member of the aminopenicillin family, incorporates an aminogroup, which aids the penetration of the drug through the outer membrane of Gram-negative bacteria allowing this β-lactam antibiotic to

kill Gram-negative bacterial cells where earlier iterations could not. The β-lactam ring of penicillins is associated with bactericidal activity, inhibiting the synthesis of the peptidoglycan layer of the bacterial cell wall by binding to penicillin binding proteins [9,10]. Resistance to ampicillin has arisen via numerous mechanisms, including the expression of β-lactamases, over production of penicillin-binding proteins, modification of outer membrane targets, membrane permeability changes, and higher antibiotic efflux expression [11,12]. This range of resistance mechanisms has made conventional antibiotics less effective, making the introduction of alternatives such as conjugated metal-based nanomaterials (including Ag-antibiotic nanoparticles) a necessity. Antibiotic conjugated metal-based nanomaterials offer a broadened spectrum of antibacterial activity, and synergistic toxicity against bacteria that enables them to circumvent antimicrobial resistance mechanisms [13,14].

An antibacterial mechanism for norvancomycin conjugated AgNPs has been proposed, where nanoparticles destabilize the outer membrane of bacterial species such as *Escherichia coli*, improving intracellular accessibility for antibiotics [15]. We propose that a similar mechanism will occur with ampicillin-conjugated AgNPs, where disruption of the outer membrane by Ag^+ ions will bypass some resistance mechanisms of Gram-negative bacteria and allow ampicillin access to the bacterial target; the penicillin-binding proteins.

This contribution investigates whether using the alternative technique of microwave heating during synthesis allows for equivalent antimicrobial activity of conjugated AgNPs against clinically isolated multidrug resistant Gram-negative bacterial species in comparison to those produced *via* conventional convection heating methods. Microwave heating methods allow for a time reduction in synthesis, thus making antibiotic capped AgNPs potentially more applicable for mass production in the pharmaceutical industry.

2. Materials and methods

2.1 Materials

Silver nitrate (204390), 14 kDa cellulose dialysis tubing (D9527), and ampicillin sodium salt (A0166) were purchased from Sigma Aldrich (UK) and used as received. Sodium borohydride (1343222) was purchased from Fisher Scientific UK Ltd.

2.2 Bacterial strains and culture conditions

Clinical isolates used in this study were obtained from the Nottingham University Hospitals Trust Pathogen Bank and are listed in Table S1. Strains were grown aerobically in Mueller-Hinton agar or broth (Merck, UK), defined minimal medium containing glucose [16], or human plasma-like medium [17,18] at 37°C. Bacterial overnight cultures were prepared by inoculating the appropriate volume of liquid medium with several colonies taken from a fresh agar plate. Cultures were incubated with 150 rpm shaking for approximately 18 h.

2.3 Genotypic identification and characterisation of clinically isolated bacterial pathogens

Genomic DNA was extracted from cell pellets using GenElute™ Bacterial Genomic DNA Kit (Merck) as per manufacturer's instructions. DNA quality was check using a NanoDrop microvolume spectrophotometer (ThermoFisher Scientific) and quantified using a Qubit 4 fluorometer (Invitrogen). Whole genome sequencing was performed on the Illumina HiSeq/NovaSeq platform by MicrobesNG (Birmingham, UK) for three strains (17Y001080, 17Y001081 and 18Y001266). Strains 21Y000039 and 21Y000040 were sequenced in-house; sequencing libraries were prepared using the Illumina DNA Prep Kit and sequenced on the Illumina MiSeq using a 2x150 cycles v2 chemistry reagent kit. Adapter sequences were trimmed from reads using Trimmomatic v0.39 (BOLGER14, [19]). Sickle v1.33 used a sliding window approach to trim reads to an average Phred quality score of Q20 (JOSHI11, [20]). Trimmed reads were assembled using SPAdes v3.15.5 (PRJIBELSKI20, [21]). Antimicrobial resistance markers were identified using Resistance Gene Identifier v6.0.0 tool of the Comprehensive Antibiotic Resistance Database v3.2.5 [22]. Genes were omitted that were identified as global regulators or two component systems where presence does not denote antibiotic resistance.Only resistance genes that showed a perfect or strict match with coverage for a given gene and thatachieved ≥90% identity and percentage length of reference sequence in the database were includedin this study.

2.4 Synthesis of sodium borohydride and ampicillin coated silver nanoparticles

Sodium borohydride reduced silver nanoparticles ($NaBH_4$-AgNPs) were synthesized from an aqueous solution of sodium borohydride ($NaBH_4$, 30 mL, 0.002 M), which was magnetically stirred on icefor 20 min. $AgNO_3$ (0.001 M, 2 mL) was added drop wise with constant stirring to the $NaBH_4$ solution at a rate of one drop per s [23]. Stirring ceased after $AgNO_3$ addition. The AgNP solution formed was dialyzed against ddH_2O (pH 5.5, <10 µS) using a 14 kDa membrane dialysis tubing for 24 h to remove excess residual reactants. Samples were freeze-dried at 223 K using a BT4KZL dryer (VirTis). Synthesis and drying were performed in the dark (samples wrapped with aluminum foil) to prevent photo-degradation of the sample.

Ampicillin coated silver nanoparticles (Amp-AgNPs) were synthesized from aqueous solutions of ampicillin (0.01 M) and $AgNO_3$ (0.01 M) that were prepared for use in the 'one-pot' synthesis approach. The solutions were mixed in a 1:1 molar ratio of ampicillin: silver nitrate, diluted with ddH_2O to a final concentration of 10^{-3} M and the final solutions heated either by water bath (B) at 40°C for 4 h for Amp-AgNPs-B [10], or microwave (M) irradiation (domestic Cookworks MS-1922H 2.45 GHz) at 100 W for 4 min for Amp-AgNPs-M. Amp-AgNPs were then dialyzed for a minimum of 1 h using 14 KDa dialysis tubing and multiple changes of water, then freeze-dried as described above for the $NaBH_4$-AgNPs.

2.5 Characterization of silver nanoparticles

The UV-Vis absorption spectra of $NaBH_4$-AgNPs and Amp-AgNPs solutions were measured using a Cary 50 Bio UV-Vis spectrophotometer (Agilent Technologies). The *zeta* potential of the AgNPs was measured using a Zetasizer Nano-S Zen 600 (Malvern Instruments Ltd.) and DTS1070 folded capillary cells (Malvern Instruments Ltd.). Both size and *zeta* potential measurements were taken at 25°C after 120 s equilibrations with water as the dispersant (η 0.8872 cP, n 1.33 and ε_r 78.5) and silver (n 0.135 and absorption 3.99) as the material. Nanoparticle size and morphology were assessed using digital micrographs obtained with a JEOL JEM-2100Plus transmission electron microscope (TEM) fitted with a LaB_6 filament, operating at an accelerating voltage of 200 kV. Samples were prepared by depositing a drop of suspended AgNPs that were initially dispersed using bovine serum albumin [24] onto 200 mesh carbon-coated grids (Quantifoil MicroTools GmbH); micrographs were taken with a Orius SC200 CCD camera (Gatan Inc.) and

analyzed in ImageJ Win64 Software. To determine the size distribution and spatial characteristics, 100 grains (from TEM) for each were used except for the sample prepared in the water bath where 500 (number of each of three different size categories (300 small, 100 medium, 100 large) grains were measured. Antibiotic loading was determined using thermogravimetric analysis (TGA) with a TGA/DSC 3+ (Mettler-Toledo International Inc.) with samples heated in air at 10°C min^{-1} over 30 - 900°C. Fourier transform infrared (FTIR) spectra were measured using a NICOLET iS50 FT-IR, with a DTGS detector and a KBr beamsplitter. The conditions used for spectral collection were: source IR, optical velocity 0.47, Aperture 87, max. range 4000 and min range 600 wavenumbers, 64 scans. X-ray diffraction (Rigaku Ultima IV X-Ray Diffractometer) revealed the domain and crystallite properties of the AgNPs. Samples were run at 40 kV and 50 mA (λ=1.540593angstroms) between 5 – 80 two theta. Scans were obtained in step mode; step size was 0.02 degreesand scan speed 5.0 deg min^{-1}.

2.6 Determination of minimal inhibitory concentrations

Minimal inhibitory concentrations (MIC) of $NaBH_4$-AgNPs, Amp-AgNPs, and ampicillin sodium were determined via the standard broth-dilution method in 96-well microtiter plates. The MICs were evaluated using 2-fold dilutions of the compounds against starter cultures diluted to an OD_{600} = 0.1 (equivalent to a 0.5 McFarland standard). Microtiter plates were incubated for 18 h at 37°C after which the presence or absence of growth in each well was recorded to determine the MIC for each antimicrobial agent.

2.7 Time-kill assays

Overnight *E. coli* cultures were diluted to a final concentration of 2.5% in 1 mL defined minimal medium containing glucose in sterile 24-well plates and incubated at 37 °C with shakingat 150 rpm. Once cultures reached an early exponential growth phase (OD_{600} ~ 0.4), Amp-AgNPs-M were added at the appropriate final concentrations, and growth was monitored at regular intervals for 5 h. Viability was measured for samples harvested at 0.5, 1, 3, 5 and 24 h post- exposure after serial dilution in phosphate-buffered saline; 5 μL aliquots were plated on Trypticase soy agar and incubated overnight at 37 °C.

2.8 Statistical analyses

GraphPad Prism v7.05 software was used for statistical analysis tests, including one-way ANOVA, two-way ANOVA with Tukey's multiple comparison tests, and Welch's t-test. Numerical data from AgNP characterization utilized Origin Pro-2023 and AgNP TEM grain measurement used ImageJ - 64-bit.

3. Results and discussion

3.1 Clinically isolated bacterial pathogens demonstrate the urgent need for new antimicrobial development

To understand the antibacterial activity of Amp-AgNPs it is important to test the antimicrobials against a range of clinically isolated pathogens. We therefore obtained five clinical isolates from the Nottingham University Hospitals Trust Pathogen Bank, with representatives isolated from wound infections and ventilator associated pneumonia cases. Strains were sequenced using Illumina technologies to confirm identity and provide draft genome sequences that could be interrogated for the presence of antimicrobial resistance genes (sequencing data available in summary Table S1). Analysis of the draft genome sequences predicted significant but varied antimicrobial resistance in all strains except *Serratia marcescens* (Fig. 1). Four out of five isolates were classified as multidrug resistant, with resistances to three or more antibiotic classes. The genotypic antibiotic resistance predictions were supported by phenotypic testing at the Nottingham University Hospitals (NUH) Pathogen Bank with *E. coli* 17Y001081 and *Klebsiella pneumoniae* 18Y001266 being most problematic, demonstrating resistance to six and 11 different antibiotic classes respectively (data not shown). The limited treatment options for these strains and the likelihood of additional resistances emerging over time demonstrates the significant threat to current antibiotic therapies and the need for new antimicrobials or antimicrobial combinations to enter development.

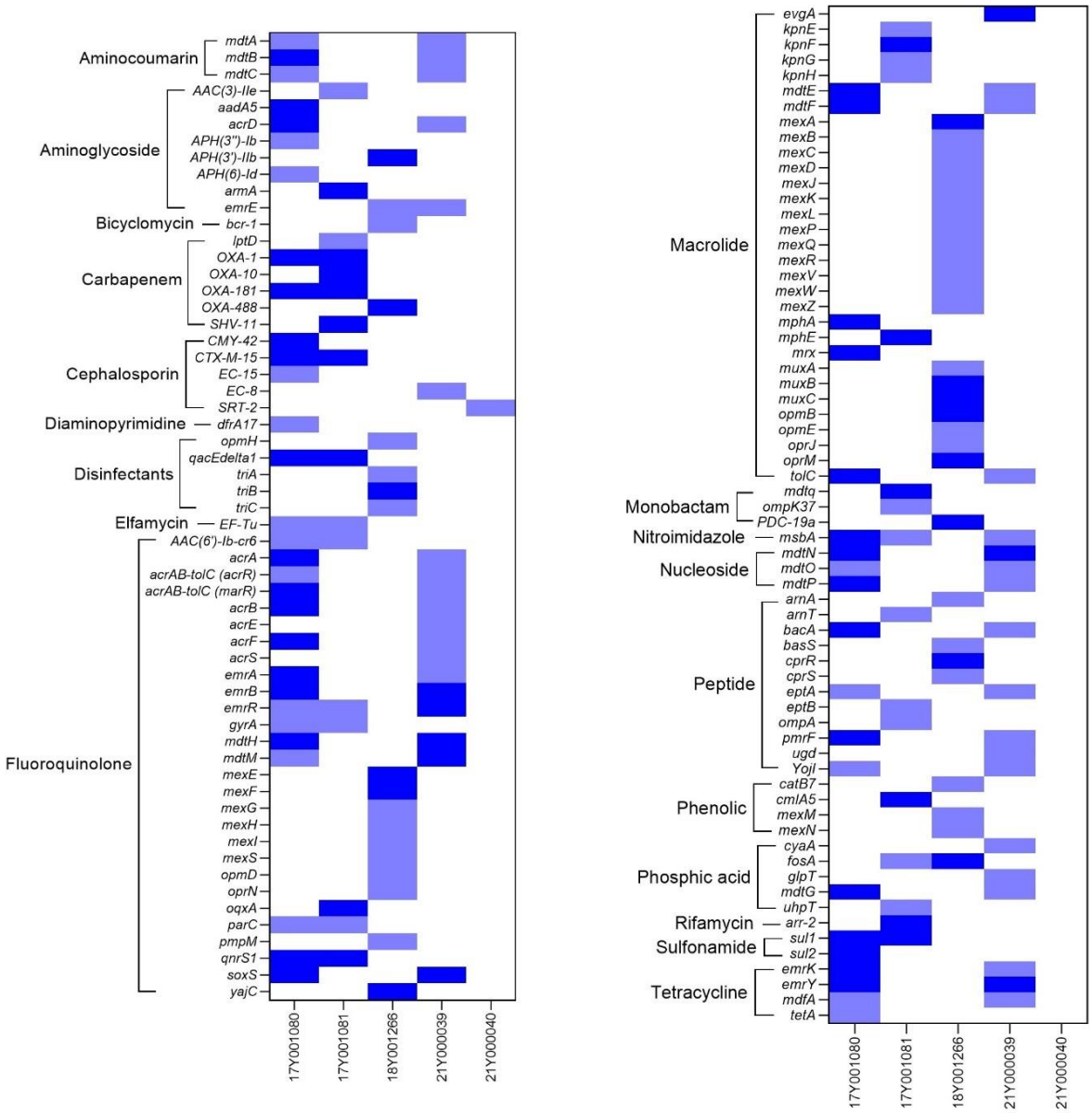

Fig. 1. Antimicrobial resistance genes predicted in the five clinical isolates using Resistance Gene Identifier v6.0.0 tool of the Comprehensive Antibiotic Resistance Database v3.2.5 [22]. White – no gene predicted, light blue – gene predicted with 90-99.99% identity, and dark blue – gene predicted with 100% identity. NUH 17Y001080: *E. coli*, NUH 17Y001081: *K. pneumoniae*, NUH 18Y001266: *Pseudomonas aeruginosa*, NUH 21Y000039: *E. coli*, and NUH 21Y000040: *S. marcescens.*

3.2 Synthesis of ampicillin-conjugated silver nanoparticles using a microwave method significantly decreases production time

The synthesis of antibiotic conjugated gold nanoparticles using a 'one-pot' approach has been demonstrated by Rai *et al.*; the same method was used to synthesize AgNPs in this study [10]. Rai *et al*. demonstrated the importance of temperature in the one-pot synthesis, where an increase in temperature was proportional to a decrease in reaction time together with a decrease in the amount of drug loaded on the nanoparticles. Heating at 40°C for 4 h yielded the least aggregated and most uniformly sized nanoparticles [10]. The one-pot method is also applicable to AgNPs and allows for AgNPs with a consistent particle size and drug load to be synthesized.

For pharmaceutical application, synthesis time is critical. Decreasing synthesis time reduces cost to companies. Therefore, we sought to determine whether the synthesis of Amp-AgNPs could be reduced using a microwave method and to understand how this altered the physical properties of the nanoparticles compared to the traditional water bath method. We synthesized and characterized the properties of Amp-AgNPs produced by both methods and compared them to sodium borohydride reduced silver nanoparticles as a control. The resultant $NaBH_4$-AgNPs, Amp-AgNPs-Bath (B) and Amp-AgNPs-Microwave (M) had characteristic yellowish, deep yellow and faintly brown colour in aqueous solution respectively (Fig. 2A, inset). The surface plasmon resonance peak (λ_{max}) shifted from around 394 nm for the $NaBH_4$-AgNPs sample to ca. 340 and 345 nm for Amp-AgNPs-B and Amp-AgNPs-M respectively. TGA analysis determined there was 34.5% silver for Amp-AgNPs-B and 36.0% silver in the Amp-AgNPs-M. The corresponding percentage of ampicillin was estimated as 60.7% for Amp-AgNPs-B and 58.6% for Amp-AgNPs-M (Fig 2B). Synthesis by the water bath method takes approximately five hours, largely due to the duration of synthesis (4 h at 40°C), whereas synthesis via the microwave method takes just over one hour, due to the short synthesis time of 4 minutes. This represents a significant time saving for production of the ampicillin-nanoparticle conjugates.

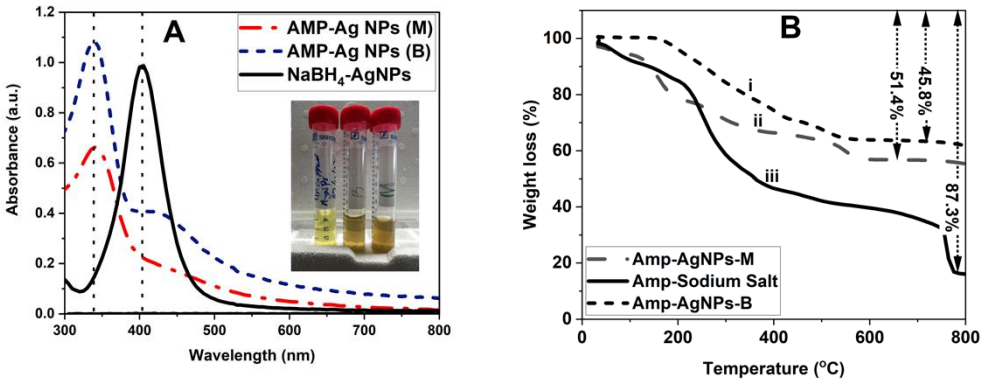

Fig. 2. (A) Visual observation of colour in the prepared nanoparticle solutions and UV-Vis absorption spectra showing the surface plasmon resonance peaks of (i) $NaBH_4$-AgNPs (black solid line), (ii) Amp-AgNPs-B (blue dotted line), and (iii) Amp-AgNPs-M (red dotted line). (B) Thermogravimetric analysis showing the percentage digestion of (i) Amp-AgNPs-M, (ii) Amp-AgNPs-B, and (iii) ampicillin sodium salt.

3.3 Antimicrobial testing demonstrates significant activity of Amp-AgNPs against a panel of clinically isolated bacterial pathogens

To understand how the differences in physical properties of the Amp-AgNPs synthesised by the two different methods effected antimicrobial activity, we tested the nanoparticle conjugates against a range of clinically isolated pathogens and to a non-pathogenic laboratory strain of *E. coli* (MG1655). Minimal inhibitory concentrations were determined for batches of AgNPs synthesised by each method alongside the equivalent concentrations of $NaBH_4$-AgNPs and ampicillin sodium. Only the laboratory control strain (MG1655) and *E. coli* 21Y000039, isolated from a ventilator-associated infection, were clinically sensitive to ampicillin, as determined by reference to the European Committee onAntimicrobial Susceptibility Testing breakpoints [25]. All other strains, isolated from either wound infections or cases of ventilator-associated pneumonia, showed extremely high levels of resistance to the antibiotic (Table 1). Many studies into the antimicrobial activity of nanometal-antibiotic conjugates have utilised rich laboratory media to demonstrate antimicrobial efficacy [26]. Use of such a rich laboratory media is helpful to provide a standard methodology that can be used to estimate the clinical outcome of treatment with an antibiotic on the market. However, when exploring new or altered drugs where no such clinical data exists the use of such rich laboratory media can be problematic for understanding the true antimicrobial potential of the drug in treatment of an infection due to potential complex interactions between the

compounds and components of the media [27]. This can lead to failure of promising drug development pipelines at costly (pre-)clinical trial stages. We therefore tested the antimicrobial efficacy of these antibiotic-AgNP conjugates in a defined minimal medium, representing areas of the body that contain few nutrients and in a human plasma-like medium that resembles the natural cellular environment found within the body, mimicking the metabolic profile of human plasma and interstitial fluid [17,18]. When compared with ampicillin sodium and $NaBH_4$-AgNP controls, the Amp-AgNPs synthesised by both the microwave and water bath methods demonstrated significantly improved inhibitory effects across all strains tested, providing clear evidence for efficacy of the Amp-AgNPs across a broad range of clinically isolated multi-drug resistant pathogens and their potential antimicrobial efficacy *in vivo* (Table 1). In a plasma-like medium, the Amp-AgNPs also demonstrated an enhanced inhibitory effect at lower concentrations of antimicrobial compared with ampicillin and $NaBH_4$-AgNP controls. In both media, the antimicrobial efficacy of the Amp-AgNPs produced by the water bath method was greater. The differences in efficacy of ampicillin, AgNPs, and Amp-AgNPs synthesized by either method are consistent with other published literature where bacterial phenotype and antimicrobial susceptibility are altered by growth in different media [28,29]. Both antibiotic efficacy and antimicrobial metal ion activity can be altered by media composition, including ion concentration and the presence of organic compounds. Components of the culture medium can influence the availability of antimicrobials, interactions with ions or nutrients, and the overall growth environment of bacteria. For example, certain nutrients or ions in the media can bind to antimicrobials, reducing their bioavailability, or interact with bacterial cells, altering susceptibility. However, whilst trends can be observed, results are bacterial strain and drug specific making them difficult to predict. This can the evidenced in the present data with lower concentrations of ampicillin required to inhibit growth of all strains in defined minimal medium compared with the more complex plasma-like medium except with *S. marcescens* where antimicrobial activity of ampicillin is higher in the complex medium (Table 1).

Table 1. Minimal inhibitory concentrations of $NaBH_4$-AgNP, Amp-AgNPs-B, Amp-AgNPs-M and ampicillin sodium in different media.

Bacterial strain	Glucose defined minimal medium				Plasma-like medium			
	Amp	$NaBH_4$-AgNP	Amp-AgNPs-M	Amp-AgNPs-B	Amp	$NaBH_4$-AgNP	Amp-AgNPs-M	Amp-AgNPs-B
***E. coli* MG1655**	**2**	**31.25**	**0.49**	**<0.24**	**64**	**500**	**7.81**	**3.91**
***E. coli*^{17Y001080}**	**4096**	**500**	**2.28**	**<0.24**	**4096+**	**500+**	**20.83**	**5.21**
***K. pneumoniae*^{17Y001081}**	**4096+**	**416.67**	**1.63**	**<0.24**	**4096+**	**500+**	**52.08**	**7.81**
***P. aeruginosa*^{18Y001266}**	**1024**	**41.67**	**0.65**	**<0.24**	**4096+**	**500+**	**15.63**	**1.95**
***E. coli*^{21Y000039}**	**0.5**	**31.25**	**0.49**	**<0.24**	**1,706.7**	**500+**	**13.02**	**5.21**
***S. marcescens*^{21Y000040}**	**4096**	**31.25**	**0.65**	**0.24**	**256**	**500+**	**10.42**	**3.91**

MIC shown in mg L^{-1}, Amp: ampicillin sodium, M: microwave synthesis, B: water bath synthesis. MG1655 is a non-pathogenic laboratory strain, isolates NUH 17Y001080, NUH 17Y001081, and NUH 18Y001266 were isolated from wound infections and isolates NUH 21Y000039, and NUH 21Y000040 were isolated from cases of ventilator-associated pneumonia.

Comparison of the antibiotic resistance genes present within the clinical pathogens (Fig. 1) and the phenotypic ampicillin resistance determined in Table 1 demonstrates the significant resistance to this β-lactam antibiotic. All highly ampicillin resistant strains have corresponding cephalosporin and/or carbapenem resistance genes present that can confer resistance to ampicillin. *E. coli* MG1655 is well known for its ampicillin sensitivity but interestingly, *E. coli* 21Y000039 shows clinical sensitivity to ampicillin despite genome analysis predicting the presence of EC-8, coding for a β-lactamase enzyme. However, with only a single gene predicted present that could confer resistance to ampicillin it could be that regulatory control of this gene is such that resistance does not occur despite its presence on the genome. The resistance to inhibition by silver nanoparticles in both complex and defined media can result from interactions between the nanoparticles and the media or from bacterial mechanisms, such as the expression of the adhesive flagellum protein flagellin that promotes nanoparticle aggregation, depression of the Cus system, loss of outer membrane porins, and expression of *sil* genes [30, 31]. Analysis of virulence factors, using the Virulence Factor Database, we identified the *ibeB* gene, responsible for cation efflux, in both pathogenic *E. coli* strains (Table S2). Flagellin production genes were also identified in *P. aeruginosa*, *E. coli* 21Y000039, and *S. marcescens*. In *K. pneumoniae*, the multidrug efflux pump genes *acrAB* were identified. In plasma-like medium, silver nanoparticle resistance suggests that components of the medium are interacting with the nanoparticles, preventing them from engaging

with bacterial cells. Notably, resistance in both media types is overcome when ampicillin is conjugated with the nanoparticles, showing significant antibacterial activity even against strains highly resistant to both ampicillin and silver nanoparticles individually.

The antimicrobial activity of Amp-AgNPs presented in Table 1, demonstrates the potential of nanometal-antibiotic complexes in treatment of multi-drug resistant bacterial infections caused by a variety of species. That these antibiotic-nanoparticle conjugates can be synthesised using the fast one-pot synthesis microwave method and still retain high levels of antimicrobial activity, much greater than ampicillin sodium or $NaBH_4$-AgNPs alone, provides a cost-effective route to scaled-up production, which is critical for pharmaceutical company buy in. The significant contrast in antimicrobial activity between nanoparticles in the absence of antibiotic and the ampicillin-conjugated nanoparticles, even in strains that are clinically resistant to ampicillin alone highlights the significant synergistic effect of administering these two antimicrobials together in a conjugated form. This opens the door to a resurgence in the use of antibiotics where resistance has emerged in combination with antimicrobials that appear to circumvent those resistance mechanisms. Repurposing older antibiotics is attractive as the safety of these molecules has been verified and their cost often lowered due to patent expiration, meaning that any pharmaceutical company investing in this technology would have lowered costs in the pathway to market.

To understand whether the inhibition of pathogens was due to killing and to determine the speed of any such killing, a time-kill assay was performed on *E. coli* 21Y000039. Here, a killing effect was identified, with a significant bactericidal effect of >2-log reduction in viability after three hours for cultures exposed to 4x and 8x the minimum inhibitory concentration (Fig. 3). Further decrease in viability was observed over 24 h, showing that subpopulations are unable to recover from the antimicrobial. Cultures exposed to 8x the minimum inhibitory concentration of Amp-AgNPs-M (3.92 mg L^{-1}) were completely killed by 24 h. By comparison, published data shows that *E. coli* exposed to silver nanoparticles alone are able to recover from concentrations as high as 80 mg L^{-1} [32], similarly strains of *E. coli*, *P. aeruginosa* and *Streptococcus pyogenes* all showed a similar pathogen recovery over 24 h when exposed to AgNPs alone [33]. This highlights the importance of nanoparticle conjugation to an antibiotic.

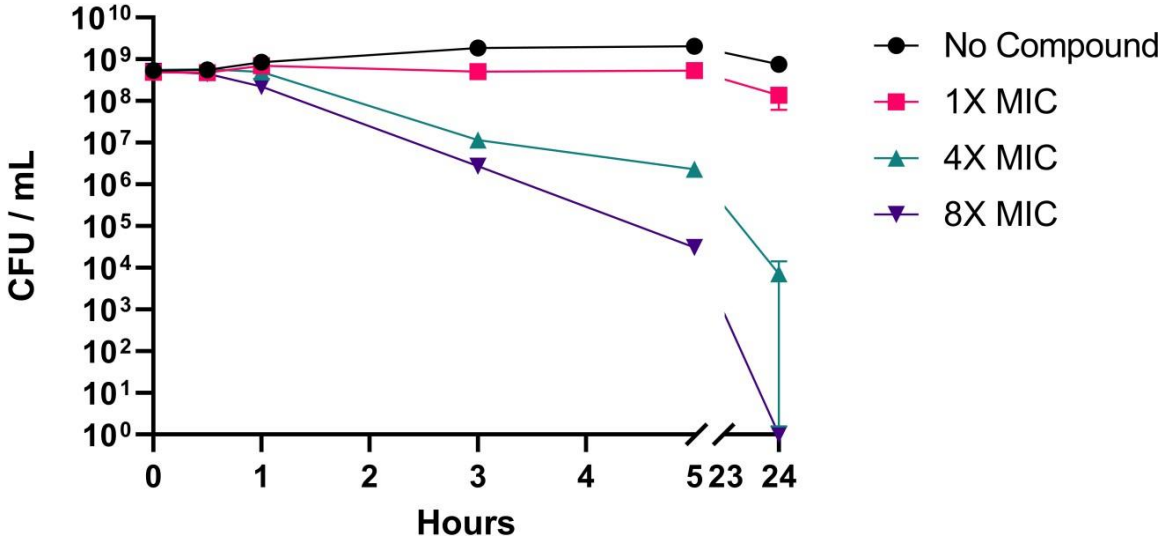

Fig. 3. Effect of Amp-AgNPs-M on the viability of *E. coli* 21Y000039 in glucose defined minimal medium. Cultures were grown to early exponential phase at 37°C and 150 rpm shaking in 250 mL with defined minimal medium containing glucose as the sole carbohydrate source. Upon reaching OD_{600} ~0.4 differing concentrations (0 – 3.92 mg L^{-1}) in accordance multiples of the MIC (0 – 8x) were added to the cultures and viability monitored through removal and dilution of culture every 30 min for 1 h and then 2 hourly until 5 h, with a final viability at 24 h. N ≥ 3 ± SD.

3.3 Synthesis conditions alter the physical properties of the ampicillin-conjugated silver nanoparticles

To better understand the difference in antimicrobial activity of Amp-AgNPs synthesized by water bath and microwave methods, the physical properties of ampicillin-conjugated silver nanoparticles were evaluated using a range of analytical tools to determine the size, charge, and interaction of the antibiotic with the nanoparticle surface.

The hydrodynamic diameter of the synthesized nanoparticles ranged from 22.30 ± 7.31 nm ($NaBH_4$-AgNPs) through to 31.57 ± 7.67 nm (Amp-Ag NPs-B) and 47.6 ± 6.4 nm (Amp-AgNPs-M) respectively (Fig. 4, Tables 2 & S3). The presence of ampicillin in the synthesis medium led to a change in charge on the nanoparticles, which is likely to impact interactions with the bacterial cell envelope.

TEM analysis showed that the AgNPs had a spherical morphology with diameter of 3.2 - 9.5 nm, 3.2 – 22.4 nm and 4.0 – 15.2 nm for $NaBH_4$-AgNPs, Amp-AgNPs-B and Amp-AgNPs-M component grains respectively (Fig. 4). Amp-AgNPs-M formed agglomerated nano balls (30.94 – 53.57 nm in diameter), each ball comprised of 15-35 component grains of diameter 4-15 nm (Fig. 4B). These grains were separated by a distance of 1.87 ± 0.4 nm, perhaps from coating of the antibiotic. The Amp-AgNPs-B sample contained particles of three distinct sizes with the smaller particles aggregating to show associated grains interspaced by a consistent distance of 1.46 ± 0.35 nm (Fig. 4C). All AgNPs showed strong crystalline signals with distinct lattice planes, and comparable d-spacing (d_{hkl} spacing) between successive planes of Ag atoms averaging 0.18 ± 0.05 nm and 0.23 nm for the most intense peak d_{hkl} (111), Fig. S1). Compared to Amp-AgNPs-M, which had a distribution of small grains between 4.0–15.2 nm, the Amp-AgNPs-B synthesized by the conventional water bath method were distributed across three distinct sizes: 6.36 ± 0.74 (small grains: ca. 90%), 12.03 ± 1.12 (medium grains: ca. 7%) and 20.71 ± 2.85 (large grains: ca. 3%). Energy dispersive X-ray analysis (EDX) confirmed the presence of silver in all samples (Fig. 4D).

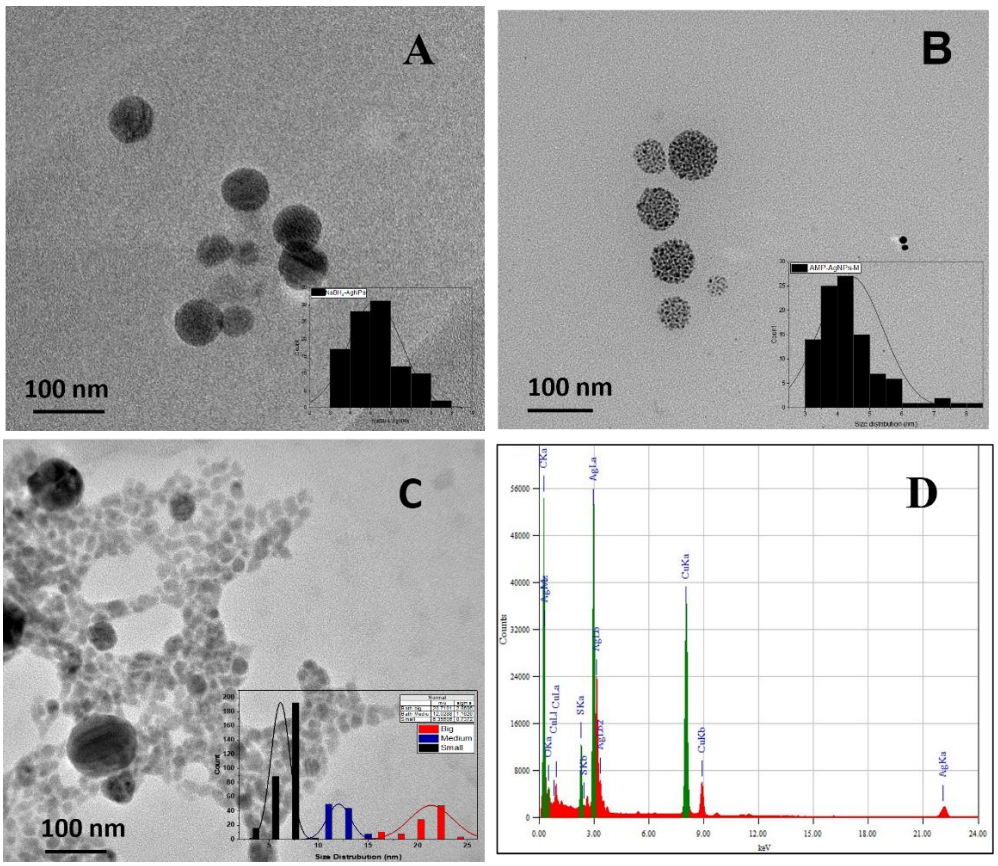

Fig. 4. Representative transmission electron microscopy (TEM) images of the AgNPs showing the morphology of (A) $NaBH_4$-AgNPs, (B) Amp-AgNPs-M, and (C) Amp-AgNPs-B. (D) is a representative energy dispersive X-ray analysis trace of elements present.

FTIR analysis was used to identify the presence of antibiotic in samples and its likely binding mode to the nanoparticles (Fig. 5). For ampicillin, FTIR bands were recorded around 3280 cm^{-1} (-OH), 1760 cm^{-1} (C=O of four membered ring lactams) and 1590 cm^{-1} (primary amine), while others (1515, 1396, and 1035 cm^{-1}) are contributions from the ß-lactam ring vibrations [10,34]. These vibrations were recorded for both the Amp-AgNP samples suggesting the integrity of the antibiotic in the composites formed by either water bath or microwave heating is retained. A shiftfrom 1590 cm^{-1} in pure ampicillin to 1500 and 1459 cm^{-1} in the Amp-AgNPs-B and Amp-AgNPs-M respectively is suggested to be due to the involvement of the primary amine of ampicillin in the nanoparticle synthesis [26].

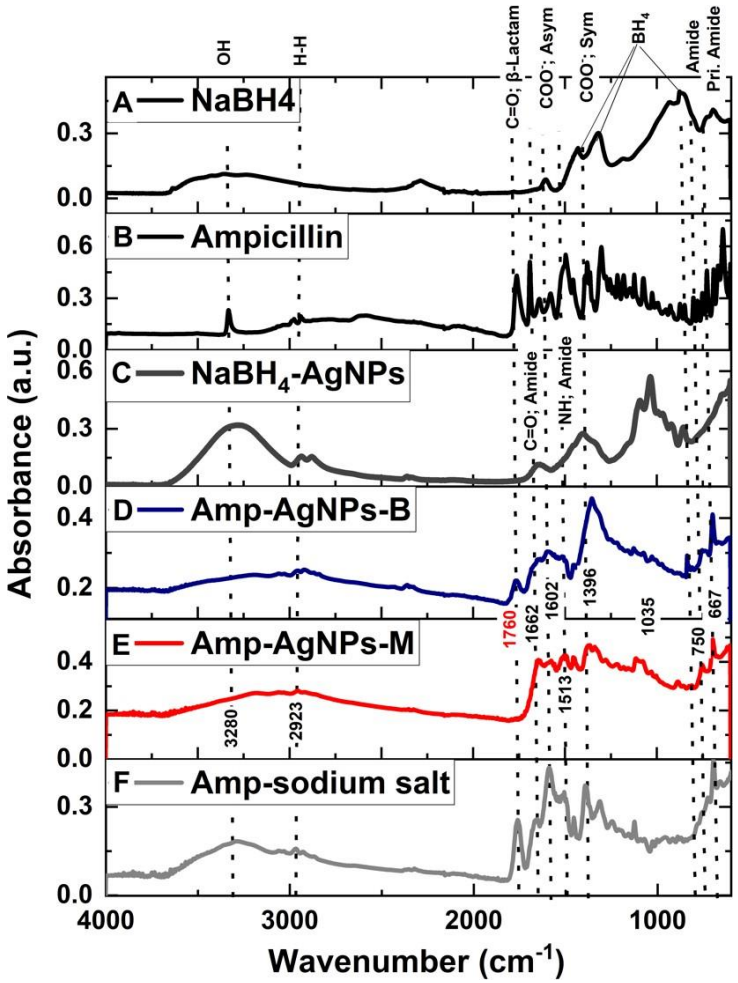

Fig. 5: Representative FTIR Spectra for (A) $NaBH_4$ (B) Ampicillin (C) NaBH4-AgNPs, (D) Amp-AgNPs-B, (E) Amp-AgNPs-M and (F) ampicillin sodium salt ($C_{16}H_{18}N_3NaO_4S$).

X-ray diffraction patterns (Fig. S3) showed the presence of silver with Miller indicescorresponding to (111), (200), (220), and (311) of face-centered cubic structure of silver (Joint Committee on Powder Diffraction Standards, File No. 4-0783). Crystallite size was calculated using the Scherrer equation $D = \frac{K\lambda}{\beta Cos\theta}$. λ denotes the wavelength (λ) of the incident X-Ray beam (1.540593 Angstrom), K is Scherrer's constant commonly taken as 0.9 [35], β represents the full width at half maximum valueof the peak, and ϴ is the Bragg angle [36,37]. The crystallite size for both Amp-AgNPs obtainedfrom XRD peaks were comparable to the hydrodynamic and grain size from DLS, and TEM, (Tables 2 & S3). The average crystallite domain size (nm) of the Amp-AgNPs-M from Scherrer'sequation were smaller (9.46 ± 4.59) compared to Amp-AgNPs-B (12.88 ± 5.62), with lower diffraction peak intensity and broader full width at half maximum. Despite being smaller, the consistent agglomeration.

of Amp-AgNPs-M into spherical balls could be responsible for the recorded functional differences of the Amp-AgNPs. For example, in a review by Díez-Pascual, it was suggested that effective surface area of AgNPs could be reduced due to agglomeration, impacting their antibacterial properties [38]. The unassigned X-ray diffraction peaks between 29 - 32 (2θ degree region) marked with asterisks are consistent with observations from previous reports and have been linkedto the crystallization of bioorganic phases on the surface of the AgNPs, this includes in plant basedAgNPs [25], fungal based AgNPs [26] and Amp-AgNPs [22]. Compared to the TEM grain size, (Table 2), the synthesized AgNPs are suggested to be largely single domains as denoted by the comparable range of values between the XRD crystallite domain size and the TEM grain sizes. The supplementary information includes the detailed crystallite properties (Table S4), size and zeta potential of the Amp-AgNPs after 8 months (Table S5), as well as the morphological characteristics (TEM) and applications of ampicillin-functionalized silver nanoparticles (Amp-AgNPs) from various studies (Table S6).

Table 2. The effect of synthesis approach on the hydrodynamic, crystal and grain sizes obtained by DLS, XRD and TEM.

Sample	**Hydrodynamic size-DLS (nm)**	**Particle size TEM (nm)**	**Average Crystallite Domain size (nm)**	**Surface *Zeta* potential (mV)**
$NaBH_4$-AgNPs	22.30 ± 7.31	3.25 -9.57	4.59 ± 1.14	-26.10 ± 3.02
Amp-AgNPs-M	33.0 ± 11.96	4.00 -15.23 (grains) 30.94-53.57 (Agglomerates)	9.46 ± 4.59	-22.80 ± 4.25
Amp-AgNPs-B	31.57 ± 7.67	3.29 – 22.45 Small grains: 6.36 ± 0.74 (ca. 90%) Medium grains: 12.03 ± 1.12 (ca. 7%) Big grains: 20.71 ± 2.85 (ca. 3%).	12.88 ± 5.62	-19.41 ± 6.13

4. Conclusions

Conjugation of ampicillin to AgNPs enhanced the antimicrobial activity achieved against a panel of multi-drug resistant bacterial pathogens isolated from wounds and patients with ventilator associated pneumonia when compared with $NaBH_4$-AgNPs or ampicillin sodium alone. The synthesis method also influenced the efficacy. Significantly, the multi-drug resistant panel of bacterial pathogens chosen are all clinically resistant to ampicillin(Antimicrobial Susceptibility Testing breakpoint for clinical resistance is 8 μg mL^{-1} in Enterobacteriaceae), with some strains being capable of growth in the highest concentrations of ampicillin tested (>4,000 μg mL^{-1}, Table 2). However, when ampicillin was conjugated to AgNPs the strains were found to be significantly more sensitive to the antibiotic, more than the additive effects of ampicillin and $NaBH_4$-AgNPs given the relatively high inhibitory concentrations for $NaBH_4$-AgNPs alone. This suggests that the multiple targets of the Amp-AgNP conjugates create a synergistic effect of enhanced antibacterial action.

The simple one-pot synthesis method for Amp-AgNPs produced *via* the microwave method produced a material that exhibited higher drug loading but overall, was a marginally less potent antimicrobial agent (Table 1). However, the continued antimicrobial efficacy of Amp-AgNP conjugates synthesised by the microwave method demonstrates the potential of this synthesis method as an alternative to the conventional water bath method that may be better suited to the large-scale manufacturing processes required for commercial application particularlygiven the reduced synthesis time. It is proposed that further research yield faster and more convenient synthesis methods would benefit the development of drug delivery *via* vectors such as nanoparticles. Examination of other antibiotic conjugated nanoparticles for their antimicrobial activity against different drug resistant pathogens and identification of other compounds tolerant of the microwave synthesis approach could provide evidence for a new class of antimicrobial drugs capable of treating multi-drug resistant infections.

CRediT authorship contribution statement

Juwon S. Afolayan (formal analysis, investigation, visualization, writing), Adam M. Varney (formal analysis, investigation, visualization, writing – review and editing), Jonathan C. Thomas (formal analysis, investigation, methodology, resources, writing – review and editing), Samantha McLean (conceptualization, formal analysis, funding acquisition, methodology, project administration, resources, visualization, writing), and Carole C. Perry (conceptualization, funding acquisition, methodology, project administration, resources, writing).

Declaration of competing interests

The authors declare no competing interests.

Data availability

The genomic data generated during the current study are available in the National Center for Biotechnology Information BioProject: PRJNA1069637. BioSample accession numbers: SAMN39617881-SAMN39617885.

Acknowledgements

The authors wish to acknowledge the contributions of R. Cullinan, D. Oliver, G.J. Hickman at Nottingham Trent University for acquisition of preliminary data.

Funding Sources

The authors are grateful to Nottingham Trent University for the award of Ph.D. studentships through the Vice Chancellors Award competition (AMV and JSA).

Abbreviations

AgNP, silver nanoparticle; TEM, transmission electron microscopy, MIC; minimum inhibitory concentration; Amp, ampicillin; DLS, dynamic light scattering; TGA/DSC, thermo-gravimetric analysis/Differential scanning calorimetry; FTIR, Fourier transform Infra-red; NUH, Nottingham University Hospital; DTGS, deuterated triglycine sulfate; Amp-AgNPs-B, ampicillin silver nanoparticles-bath; Amp-AgNPs-M; ampicillin silver nanoparticles-microwave; $NaBH_4$, sodium borohydride; $NaBH_4$-AgNPs, sodium borohydride reduced silver nanoparticles; XRD, X-ray Diffraction; ANOVA, analysis of variance;; MDR, multi-drug resistance; OD, Optical density; CCD, charge-coupled device; JEOL, Japan Electron Optics Laboratory.

References

[1] J.W. Alexander, History of the medical use of silver, Surg Infect (Larchmt) 10 (2009) 289–292. https://doi.org/10.1089/sur.2008.9941.

[2] N. Silvestry-Rodriguez, E.E. Sicairos-Ruelas, C.P. Gerba, K.R. Bright, Silver as a disinfectant, Rev Environ Contam Toxicol 191 (2007) 23–45. https://doi.org/10.1007/978-0-387-69163-3_2.

[3] J. Davies, D. Davies, Origins and evolution of antibiotic resistance, Microbiology and Molecular Biology Reviews 74 (2010) 417–433. https://doi.org/10.1128/MMBR.00016-10.

[4] D. Thomas, C. Wessel, The State of Innovation in Antibacterial Therapeutics, 2022. https://www.bio.org/sites/default/files/2022-02/The-State-of-Innovation-in-Antibacterial-Therapeutics.pdf (accessed September 28, 2022).

[5] M.H. Todd, D.M. Klug, F.I.M. Idiris, M.A.T. Blaskovich, F. von Delft, C.G. Dowson, C. Kirchhelle, A.P. Roberts, A.C. Singer, There is no market for new antibiotics: This allows an open approach to research and development, Wellcome Open Res 6 (2021) 1–14.

[6] A. Sharma, A. Singh, M.A. Dar, R.J. Kaur, J. Charan, K. Iskandar, M. Haque, K. Murti, V. Ravichandiran, S. Dhingra, Menace of antimicrobial resistance in LMICs: Current surveillance practices and control measures to tackle hostility, J Infect Public Health 15 (2022) 172–181.

[7] A. Frei, J. Zuegg, A.G. Elliott, M. Baker, S. Braese, C. Brown, F. Chen, C. G. Dowson, G. Dujardin, N. Jung, A.P. King, A.M. Mansour, M. Massi, J. Moat, H.A. Mohamed, A.K. Renfrew, P.J. Rutledge, P.J. Sadler, M.H. Todd, C.E. Willans, J.J. Wilson, M.A. Cooper,

M.A.T. Blaskovich, Metal complexes as a promising source for new antibiotics, Chem Sci 11 (2020) 2627–2639. https://doi.org/10.1039/c9sc06460e.

[8] A. Majdalawieh, M.C. Kanan, O. El-Kadri, S.M. Kanan, Recent advances in gold and silver nanoparticles: Synthesis and applications, J Nanosci Nanotechnol 14 (2014) 4757–4780. https://doi.org/10.1166/jnn.2014.9526.

[9] J.F. Fisher, S.O. Meroueh, S. Mobashery, Bacterial resistance to β-lactam antibiotics: Compelling opportunism, compelling opportunity, Chem Rev 105 (2005) 395–424. https://doi.org/10.1021/cr030102i.

[10] A. Rai, A. Prabhune, C.C. Perry, Antibiotic mediated synthesis of gold nanoparticles with potent antimicrobial activity and their application in antimicrobial coatings, J Mater Chem 20 (2010) 6789. https://doi.org/10.1039/c0jm00817f.

[11] M. Li, Q. Liu, Y. Teng, L. Ou, Y. Xi, S. Chen, G. Duan, The resistance mechanism of Escherichia coli induced by ampicillin in laboratory , Infect Drug Resist Volume 12 (2019) 2853–2863. https://doi.org/10.2147/IDR.S221212.

[12] S. Ono, T. Muratani, T. Matsumoto, Mechanisms of Resistance to Imipenem and Ampicillin in *Enterococcus faecalis*, Antimicrob Agents Chemother 49 (2005) 2954–2958. https://doi.org/10.1128/AAC.49.7.2954-2958.2005.

[13] E. Sánchez-López, D. Gomes, G. Esteruelas, L. Bonilla, A.L. Lopez-Machado, R. Galindo, A. Cano, M. Espina, M. Ettcheto, A. Camins, A.M. Silva, A. Durazzo, A. Santini, M.L. Garcia, E.B. Souto, Metal-Based Nanoparticles as Antimicrobial Agents: An Overview, Nanomaterials 10 (2020) 292. https://doi.org/10.3390/nano10020292.

[14] A.S. Dove, D.I. Dzurny, W.R. Dees, N. Qin, C.C. Nunez Rodriguez, L.A. Alt, G.L. Ellward, J.A. Best, N.G. Rudawski, K. Fujii, D.M. Czyż, Silver nanoparticles enhance the efficacy of aminoglycosides against antibiotic-resistant bacteria, Front Microbiol 13 (2023). https://doi.org/10.3389/fmicb.2022.1064095.

[15] Q. Wei, J. Ji, J. Fu, J. Shen, Norvancomycin-capped silver nanoparticles: Synthesis and antibacterial activities against E. coli, Sci China B Chem 50 (2007) 418–424. https://doi.org/10.1007/s11426-007-0028-6.

[16] A.M. Varney, K.L. Smitten, J.A. Thomas, S. Mclean, Transcriptomic Analysis of the Activity and Mechanism of Action of a Ruthenium(II)-Based Antimicrobial That Induces Minimal Evolution of Pathogen Resistance, ACS Pharmacol Transl Sci 4 (2021) 168–178. https://doi.org/10.1021/acsptsci.0c00159.

[17] T. Ackermann, S. Tardito, Cell Culture Medium Formulation and Its Implications in Cancer Metabolism, Trends Cancer 5 (2019) 329–332. https://doi.org/10.1016/j.trecan.2019.05.004.

[18] J. Vande Voorde, T. Ackermann, N. Pfetzer, D. Sumpton, G. Mackay, G. Kalna, C. Nixon, K. Blyth, E. Gottlieb, S. Tardito, Improving the metabolic fidelity of cancer models with a

physiological cell culture medium, Sci Adv 5 (2019). https://doi.org/10.1126/sciadv.aau7314.

[19] A.M. Bolger, M. Lohse, B. Usadel, Trimmomatic: a flexible trimmer for Illumina sequence data, Bioinformatics 30 (2014) 2114–2120. https://doi.org/10.1093/bioinformatics/btu170.

[20] N. Joshi, J. Fass, Sickle: A sliding-window, adaptive, quality-based trimming tool for FastQ files (Version 1.33) , Https://Github.Com/Najoshi/Sickle (2011).

[21] A. Prjibelski, D. Antipov, D. Meleshko, A. Lapidus, A. Korobeynikov, Using SPAdes De Novo Assembler, Curr Protoc Bioinformatics 70 (2020). https://doi.org/10.1002/cpbi.102.

[22] B.P. Alcock, W. Huynh, R. Chalil, K.W. Smith, A.R. Raphenya, M.A. Wlodarski, A. Edalatmand, A. Petkau, S.A. Syed, K.K. Tsang, S.J.C. Baker, M. Dave, M.C. McCarthy, K.M. Mukiri, J.A. Nasir, B. Golbon, H. Imtiaz, X. Jiang, K. Kaur, M. Kwong, Z.C. Liang, K.C. Niu, P. Shan, J.Y.J. Yang, K.L. Gray, G.R. Hoad, B. Jia, T. Bhando, L.A. Carfrae, M.A. Farha, S. French, R. Gordzevich, K. Rachwalski, M.M. Tu, E. Bordeleau, D. Dooley, E. Griffiths, H.L. Zubyk, E.D. Brown, F. Maguire, R.G. Beiko, W.W.L. Hsiao, F.S.L. Brinkman, G. Van Domselaar, A.G. McArthur, CARD 2023: expanded curation, support for machine learning, and resistome prediction at the Comprehensive Antibiotic Resistance Database, Nucleic Acids Res 51 (2023) D690–D699. https://doi.org/10.1093/nar/gkac920.

[23] M.U. Rashid, Md.K.H. Bhuiyan, M.E. Quayum, Synthesis of Silver Nano Particles (Ag-NPs) and their uses for Quantitative Analysis of Vitamin C Tablets, Dhaka University Journal of Pharmaceutical Sciences 12 (2013) 29–33. https://doi.org/10.3329/dujps.v12i1.16297.

[24] B. Michen, C. Geers, D. Vanhecke, C. Endes, B. Rothen-Rutishauser, S. Balog, A. Petri-Fink, Avoiding drying-artifacts in transmission electron microscopy: Characterizing the size and colloidal state of nanoparticles, Sci Rep 5 (2015). https://doi.org/10.1038/srep09793.

[25] The European Committee on Antimicrobial Susceptibility Testing, Breakpoint tables for interpretation of MICs and zone diameters, version 12.0, (2023). http://www.eucast.org/clinical_breakpoints/.

[26] N. Khatoon, H. Alam, A. Khan, K. Raza, M. Sardar, Ampicillin Silver Nanoformulations against Multidrug resistant bacteria, Sci Rep 9 (2019) 1–10. https://doi.org/10.1038/s41598-019-43309-0.

[27] J. Rewak-Soroczynska, A. Dorotkiewicz-Jach, Z. Drulis-Kawa, R.J. Wiglusz, Culture Media Composition Influences the Antibacterial Effect of Silver, Cupric, and Zinc Ions against *Pseudomonas aeruginosa*, Biomolecules 12 (2022) 963. https://doi.org/10.3390/biom12070963.

[28] A.M. Varney, E. Mannix-Fisher, J.C. Thomas, S. McLean, Evaluation of phenotypic and genotypic methods for the identification and characterization of bacterial isolates recovered from catheter-associated urinary tract infections, Journal of Applied Microbiology, Volume 135, Issue 7, lxae155, https://doi.org/10.1093/jambio/lxae155.

[29] J. Rewak-Soroczynska, A. Dorotkiewicz-Jach, Z. Drulis-Kawa, R.J. Wiglusz, Culture Media Composition Influences the Antibacterial Effect of Silver, Cupric, and Zinc Ions against *Pseudomonas aeruginosa*, Biomolecules. 9;12(7):963. doi:

10.3390/biom12070963. PMID: 35883519; PMCID: PMC9312735.

[30] Panáček, A., Kvítek, L., Smékalová, M. et al. Bacterial resistance to silver nanoparticles and how to overcome it. Nature Nanotech 13, 65–71 (2018). https://doi.org/10.1038/s41565-017-0013-y.

[31] C.P. Randall, A. Gupta, N. Jackson, D. Busse, A.J. O'Neill. Silver resistance in Gram-negative bacteria: a dissection of endogenous and exogenous mechanisms, J Antimicrob Chemother, 70(4) (2015) 1037-46. doi: 10.1093/jac/dku523.

[32] M.A. Haque, R. Imamura, G.A. Brown, V.R. Krishnamurthi, I.I. Niyonshuti, T. Marcelle, L.E. Mathurin, J. Chen, Y. Wang, An experiment-based model quantifying antimicrobial activity of silver nanoparticles on *Escherichia coli*, RSC Adv 7 (2017) 56173–56182. https://doi.org/10.1039/C7RA10495B.

[33] H.H. Lara, N. V. Ayala-Núñez, L. del C. Ixtepan Turrent, C. Rodríguez Padilla, Bactericidal effect of silver nanoparticles against multidrug-resistant bacteria, World J Microbiol Biotechnol 26 (2010) 615–621. https://doi.org/10.1007/s11274-009-0211-3.

[34] A. Rogowska, K. Rafińska, P. Pomastowski, J. Walczak, V. Railean-Plugaru, M. Buszewska-Forajta, B. Buszewski, Silver nanoparticles functionalized with ampicillin, Electrophoresis 38 (2017) 2757–2764. https://doi.org/10.1002/elps.201700093.

[35] P. Scherrer, Determination of the size and internal structure of colloidal particles using X-rays, News from the Society of Sciences in Göttingen, Mathematical-Physical Class (1918) 98–100.

[36] P. Debye, P. Scherrer, Interference on inordinate orientated particles in x-ray light., Physikalische Zeitschrift 18 (1917) 291–301.

[37] P. Debye, P. Scherrer, Interference of irregularly oriented particles in x-rays, Physikalische Zeitschrift 17 (1916) 277–283.

[38] A.M. Díez-Pascual, Antibacterial Action of Nanoparticle Loaded Nanocomposites Based on Graphene and Its Derivatives: A Mini-Review, Int J Mol Sci 21 (2020) 3563. https://doi.org/10.3390/ijms21103563.